Accepted Manuscript

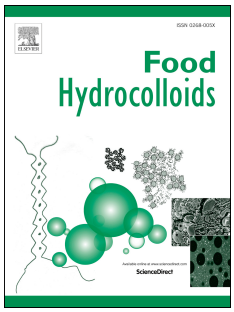

Betanin loaded nanocarriers based on quinoa seed 11S globulin. Impact on the protein structure and antioxidant activity

Jimena H. Martínez, Francisco Velázquez, Hernán P. Burrieza, Karina D. Martínez, A. Paula Domínguez Rubio, Cristina dos Santos Ferreira, María del Pilar Buera, Oscar E. Pérez

PII: S0268-005X(18)30400-4

DOI: 10.1016/j.foodhyd.2018.09.016

Reference: FOOHYD 4653

To appear in: *Food Hydrocolloids*

Received Date: 5 March 2018

Revised Date: 1 September 2018

Accepted Date: 10 September 2018

Please cite this article as: Martínez, J.H., Velázquez, F., Burrieza, Hernán.P., Martínez, K.D., Paula Domínguez Rubio, A., dos Santos Ferreira, C., del Pilar Buera, Marí., Pérez, O.E., Betanin loaded nanocarriers based on quinoa seed 11S globulin. Impact on the protein structure and antioxidant activity, *Food Hydrocolloids* (2018), doi: https://doi.org/10.1016/j.foodhyd.2018.09.016.

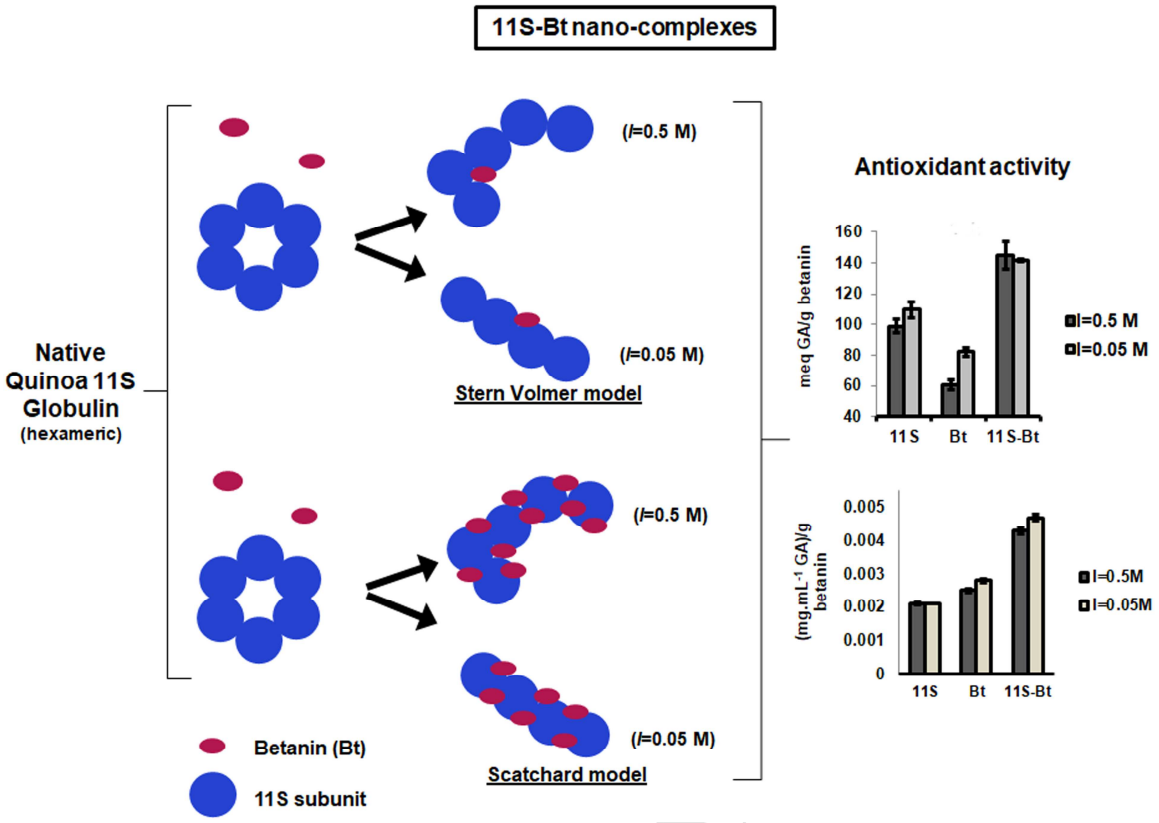

~~**Nanocolloid for the bioactive betanin based on purified 11S globulin from Quinoa seed. Impact on the protein structure and antioxidant activity**~~

Betanin loaded nanocarriers based on quinoa seed 11S globulin. Impact on the protein structure and antioxidant activity.

Jimena H. Martínez [a,b], Francisco Velázquez[a,b], Hernán P.Burrieza[c,d], Karina D Martínez [e,g], A. Paula Domínguez Rubio [a,b], Cristina dos Santos Ferreira[f], María del Pilar Buera[e,g] and Oscar E. Pérez*[a,b,h]*

[a]Universidad de Buenos Aires, Facultad de Ciencias Exactas y Naturales, Departamento de Química Biológica, Buenos Aires, Argentina.

[b] CONICET, Universidad de Buenos Aires, Instituto de Química Biológica de la Facultad de Ciencias Exactas y Naturales (IQUIBICEN), Buenos Aires, Argentina.

[c] Universidad de Buenos Aires, Facultad de Ciencias Exactas y Naturales, Departamento de Biodiversidad y Biología Experimental, Buenos Aires, Argentina.

[d] CONICET, Universidad de Buenos Aires, Instituto de Biodiversidad y Biología Experimental y Aplicada (IBBEA), Buenos Aires, Argentina.

[e]Universidad de Buenos Aires, Facultad de Ciencias Exactas y Naturales, Departamento de Industrias, Buenos Aires, Argentina.

[f]Universidad de Buenos Aires, Facultad de Ciencias Exactas y Naturales, Departamento de Química Orgánica, Buenos Aires, Argentina.

[g]CONICET. Universidad de Buenos Aires, Instituto de Tecnología de Alimentos y Procesos Químicos (ITAPROQ), Buenos Aires Argentina.

[h] Departamento de Desarrollo Productivo y Tecnológico, Universidad Nacional de Lanús, Provincia de Buenos Aires, Argentina

*Corresponding authors: Dr. María del Pilar Buera and Dr. Oscar E. Pérez.

Tel: +54 11 45763342; fax: +54 11 45763342.

E-mail addresses: pilar@di.fcen.uba.ar; oscarperez@qb.fcen.uba.ar

ABSTRACT

The objective of the present contribution was to design and characterize betanin (Bt) loaded in a nanovehicle of 11S quinoa seed protein. 11S was isolated from quinoa seed floor. Protein purification was performed by Size-Exclusion Chromatography. MALDI-TOF (Matrix-Assisted Laser Desorption/Ionization-Time-Of-Flight) analysis confirmed the identity of 11S. Nanocarriers (11S-Bt) were generated at pH 8 at different ionic strength. Globulin intrinsic fluorescence spectra showed a quenching effect exerted by Bt, demonstrating in turn protein-bioactive interaction. Stern-Volmer and Scatchard models application confirmed static quenching and allow obtaining parameters that described 11S and betanincomplexation process. Bt-11S globulin interactions seem to be more probably of physical type. Protein solubility was increasedafter complexation with Bt. 11S betanin-loaded nanocarrier showed additive effect in terms of both, antiradical or reducing power capacity in comparison to Bt as evaluated by two methods, 2,2 -azino-bis-(3-ethylbenzothiazoline-6-sulfonate) (ABTS), and by ferric reducing antioxidant power (FRAP). Interestingly 11S globulin quaternary structure was modified by the bioactive, experimenting hexamer dissociation. This nanocolloid could have the potentiality to exert the Bt controlled delivery for pharmaceutical and nutraceutical products. Bt could also be protected from light and oxygen in such systems.

Keywords: 11S quinoa globulin; betanin; antioxidant activity; nanocarrier.

1. INTRODUCTION

Quinoa (*Chenopodium quinoa* Willd.) is an ancestral crop native to the Andean regions of South America. Quinoa seeds has been revaluated ~~rediscovered~~ in recent years because of its nutritional properties, for instance proteins with high nutritional value and the presence of antioxidants molecules (Bois, Winkel, Lhomme, Raffaillac, & Rocheteau, 2006; Burrieza, Koyro, Tosar, Kobayashi, & Maldonado, 2012; Jacobsen, Mujica, & Jensen, 2003; Sanchez, Lemeur, Damme, & Jacobsen, 2003). Antioxidant properties of quinoa seed extracts have been studied by Park et al, 2017, comparing crops from Korea, USA and Peru and they found differences among them according to the assay employed to measure different metabolites with antioxidant capacity (Park, Lee, Kim, & Yoon, 2017).The nutritional value of this pseudocereal has always been highlighted, as it contains an excellent balance of amino acids and essential fatty acids, being also rich in vitamins and minerals. Quinoa seeds possesses high amount of lysine, an essential aminoacid for humans (Nowak, Du, & Charrondière, 2016). Thus, the seed technological potential lays on its components, in particular its proteins, pigments and antioxidants (Tang, Li, Chen, et al., 2015; Tang, Li, Zhang, et al., 2015).

Quinoa 11S globulin, also referred to as chenopodin, is one of the major seed storage proteins and has a similar structure to glycinin, the 11S globulin of soy. 11S is a hexamer consisting of six pairs of acid and/or basic polypeptides at pH 8 (Adachi et al., 2003). The acid and basic polypeptides have molecular weights ranging from 20 to 25 kDa and 30–40 kDa, respectively, and they are linked to each other by disulphide bonds (Abugoch et al., 2009; Ruiz, Xiao, Van Boekel, Minor, & Stieger, 2016).

On the other hand, betalains are water-soluble nitrogen-containing pigments derived from tyrosine via betalamic acid. Among betalains, betacyanins range from red to violet and betaxanthines from yellow to orange (Gandía-Herrero, Escribano, & García-Carmona, 2010a). Betalains extracted from various vegetal sources demonstrated to have antioxidant capacity (Escribano, 1998; Pedreño

&Escribano, 2001). ~~Betanin (Bt) is one of the well-characterized betacyaninobtained from red beet (*Beta vulgaris* L.), with a typical red color~~. Structurally, Bt is composed of the aglyconebetanidin which is linked by a β-glycosidic linkage with a glucose-unit at C5 (Strack, Vogt, & Schliemann, 2003). On the basis of literature data, it can be mentioned that Bt is a food and cosmetic colorant with biological activity (Esatbeyoglu, Wagner, Schini-Kerth, & Rimbach, 2015a).

Protein molecules can form superstructures by self-assembly. This term alludes to the spontaneous union of molecules in response to extrinsic changes such as: pH, ionic strength (I), temperature and /or concentration and their union with ligands (Gan & Wang, 2007; Ichikawa, Iwamoto, & Watanabe, 2005). These structures are studied by Nanotechnology, which is a field in expansion in the food and pharmaceutical industries, which is especially important in the field of nanoencapsulation (Faridi Esfanjani & Jafari, 2016) and nanocarriers (Abaee, Mohammadian, & Jafari, 2017).Biopolymer nanoparticles constituted in this way can be used for encapsulating, protecting, and realizing bioactive agents, or to alter texture, stability or appearance of products (Jafari & McClements, 2017). When aggregates bind to organic molecules of different chemical nature, they form complexes, composed by the protein and the ligand. Thus, a new structure is obtained, the nanocarriers, with enormous potential to act as a nanovehicles adsorbing different ligand compounds, with dimensions <100 nm and presenting a high surface/mass ratio.

One of the most interesting features of these nanocarriers is their potential to entrap and release compounds previously loaded, such as Bt in our case. This release process could be modulated by the pH medium, temperature or I (Pérez et al., 2014). In this context, several attempts have been made to develop nanovehicles, via nano-complexation systems and subsequent site-specific release of compounds with biological importance in pharmaceutical, nutraceutical and food industries, using proteins as nano-encapsulating agents (Nasti et al., 2009).

GRAS (Generally Recognized as Safe) phytochemicals are commonly used for the health benefits they offer. Many phytochemicals are poorly absorbed by the human body; thus one of the most

106 important and interesting applications of phytochemicals encapsulation in nano-vehicles is to
107 enhance their bioavailability by changing the pharmacokinetics and bio-distribution. To improve
108 nutritional quality and stability of the bioactive compound, one option is to encapsulate the
109 functional components using biocompatible materials that can exhibit controlled release behavior
110 (Huang, Yu, & Ru, 2010).
111 Thus, the objective of the present contribution was to design and to characterize Bt loaded 11S
112 globulin from quinoa seed vehicles designed into the nanoscale, i.e. nanocarriers. Crucial parameters
113 for 11S-Bt nanovehicles, such as the apparent binding constant and the number of binding sites on
114 the protein were evaluated by applying different mathematical models to fluorescence experimental
115 data. The antioxidant capacity of nanocarriers was also evaluated. According to our knowledge, the
116 possibility of generating this kind of nanocarriersfor Bt, has not been studied, at least into the context
117 of maximum protein solubility.
118

119 **2. MATERIALS AND METHODS**

120 **2.1 Materials**

121 Bolivian quinoa “red type” seeds were obtained from a local supermarket at Buenos Aires City,
122 Argentina. Protein content of seeds was 14.1 ± 0.2% (Nx6.25), determined by Kjeldahl method
123 (Iswaran, V., & Marwah, 1980). 11S globulin was isolated from the defatted quinoa seed flour
124 according to the method proposed by Brinegar & Goundan, (1993) modified by Quiroga et al.,
125 (2007). Briefly, 10 g of defatted flour was stirred into the extraction buffer (0.5M NaCl, 50 mMTris-
126 HCl, pH 8) for 1 h at 20°C. Then albumin fraction was removed by centrifugation at 10,000 x g for
127 10 min at 5°C. This first pellet was discarded and the supernatant adjusted to pH 5 with 10% of
128 acetic acid and centrifuged under the same conditions. This second pellet, enriched in 11S was
129 resuspended into 12 ml of extraction buffer and centrifuged as before. The resulting pellet was
130 discarded and the third supernatant, containing mainly the native 11S globulin, was filtered through

131 0.45 µm (Whatman International Ldt, Maidstone, England) and then submitted to a chromatography
132 separation process.
133 Bt was purchased from Sigma-Aldrich Chemical Co. (CDS000584) and used without further
134 purification. All chemicals were of analytical grade and Milli-Q water was always used.
135

136 **2.2. Methods**

137 **2.2.1. 11S purification**

138 An ÄKTA Protein Purification System, FPLC, (GE Healthcare Life Sciences, Germany) appliance
139 was used. It was equipped with Sephadex® S200 10/300 GL (GE Healthcare Life Sciences, Uppsala,
140 Sweden) column. Aliquots of 2 ml containing the total globulins equilibrated for 12 h at 20°C were
141 submitted to size exclusion chromatography process. Samples were eluted with extraction buffer, pH
142 8, NaCl 0.5M and at a flow rate of 1 ml/min at 25°C. Fractions of 2.5 ml were collected and analyzed
143 by absorbance at 280 nm. The eluted fraction corresponding to 11S globulin was lyophilized for 24 h
144 in a Stokes freeze-dryer (Barber-Colman, Philadelphia PA 19120, USA). Finally, samples were
145 stored at -20°C up to the moment in which they were employed.

146 **2.2.2. SDS-PAGE Electrophoresis**

147 The fraction corresponding to total globulins and those samples collected from chromatography were
148 analyzed in SDS-PAGE according to Laemmli (1970). To this end, a Mini-Protean II device (Bio-
149 Rad, CA, USA) was used. 12% of polyacrylamide running gels was used under denaturing
150 conditions at 90 V. 40 mg of protein was deposited in each well. After electrophoresis, a Coomassie
151 brilliant blue staining to detect proteins was performed (Neuhoff, Arold, Taube, & Ehrhardt, 1988).

152 **2.2.3. Protein identification**

Extracted proteins obtained from quinoa seed were digested with trypsin and analyzed by nano-HPLC coupled to mass spectrometry with Orbitrap technology (LC-MS) (Wada H. et al., 2014). The bands were excised from the gel, minced, washed with distilled water and distained using 50 mM ammonium bicarbonate (ABC) and 25mM, 50% acetonitrile (ACN) until blue color was completely removed. Samples were dried with ACN 100% before the reduction step.

Reduction and alkylation was performed with 50µL of 10 mM DTT in 50 mM ABC for 30 min at 60 °C. Then, 35µL of 55 mM Iodoacetamide in 50 mM ABC was added. Samples were incubated in the dark for 30 min at room temperature. Samples were washed with ABC 50mM, followed by 25 mM ABC, 50% ACN and then dried with 100% ACN before digestion. Samples were re-hydrated with 10 mM acetic acid with trypsin (10ng/µL) on ice, 25mM ABC was then added and digestion was performed overnight at 37 °C. Samples were cleaned and peptides extracted with Zip-Tip C18. Samples were analyzed by HPLC (Thermo Scientific EASY-nLC 1000 chromatographer/ C18 reverse phase Easy-Spray Column PepMap RSLC [P/N ES803]) coupled to electrospray ionization mass spectrometry (Thermo Scientific Electrospray EASY-SPRAY/ Q-Exactive mass spectrometer) by MS and MS/MS of the predominant peaks. Chromatograms were analyzed using Proteome Discoverer v. 2.1 Thermo Scientific. MS/MS spectra data sets were compared with Quinoa Genome Database (Yasui et al., 2016). The results were manually analyzed: only proteins identified with more than 2 peptides were taken into consideration.

2.2.4. Design of Bt loaded 11S nanocarriers

Powder samples of 11S globulin and Bt were dissolved separately in the appropriate buffers to give I= 0.5M or I=0.05M, pH 8 at room temperature under gently agitation. Sample pH was adjusted to 8.0 using 1M NaOH. At this pH value the protein solubility was maximum (Brinegar & Goundan, 1993; Quiroga et al., 2007). The solutions were prepared freshly, filtered through 0.45 µm microfilters (Whatman International Ldt, Maidstone, England) and kept at 4°C for 24 h to achieve

178 the complete hydration of the molecules. Mixed solutions were produced by mixing the appropriate
179 volume of the double concentrated 11S and Bt solutions, to give the required final concentrations.
180 The final protein concentration was kept constant at 0.1%, w/w, meanwhile Bt concentration ranged
181 0.05 - 1 % w/w. Protein concentration in the filtrate was determined by the Kjeldahl method with no
182 change in its content ($p<0.01$).

183 **2.2.5. Protein Solubility**

184 0.2% w/w 11S globulin solutions were prepared and then diluted to 0.1 % w/w. Mixed solutions
185 were prepared as indicated in 2.2.4. Single protein or 11S-Bt solutions were centrifuged at 100,000 x
186 g for 30 min at room temperature in a SW 50.1 rotor (Beckman Optima L-80, Beckman Coulter,
187 United States). Protein concentration, before (C_0), and after centrifugation (C) were quantified by the
188 Bradford assay. Solubility was expressed as Nishinari, Fang, Guo, & Phillips (2014):

189

190 $$\text{Solubility \%} = (C/C_0)*100 \qquad (1)$$

191

192 **2.2.6. Particle size and ζ-potential determinations**

193 Dynamic light scattering (DLS) experiments were carried out in a dynamic laser light scattering
194 (DLS) (Zetasizer Nano-Zs, Malvern Instruments, Worcestershire, United Kingdom) provided with a
195 He-Ne laser (633 nm) and a digital correlator, Model ZEN3600. Measurements were carried out at a
196 fixed scattering angle of 173º. Samples were contained in a disposable polystyrene cuvette. Samples
197 were contained in a disposable polystyrene cuvette, measurements were carried out at 25ºC, with the
198 water (the dispersant) refractive index, which was equal to 1.333; dielectric constant of 78.5;
199 viscosity of 0.8872 cp, and equilibration time was always 180 s. Analysis of these intensity
200 fluctuations yields the diffusion coefficient of the particle and hence the particle size using de
201 Stokes-Einstein. Results were interpreted as in Pérez et al. (2014)~~equation (2):~~

202

~~dH= k.T/6.π.η.D (2)~~

~~Size information data for percentile distribution of particle/aggregate sizes was obtained by using a multi exponential function (CONTIN) to fit the correlation data. Through Mie theory, it is possible to convert the intensity distribution to volume distribution (Pérez et al., 2014).~~

Bt concentrations considered in mixed solutions ranged from 0.05 to 1%, w/w for the DLS analysis.

~~2.2.7 ζ potential measurements~~

ζ–potential measurements were also performed in the same DLS instrument ~~(Zetasizer Nano–Zs, Malvern Instruments, Worcestershire, United Kingdom)~~. The ζ–potential was evaluated from the electrophoretic mobility of the particles. The conversion of the measured electrophoretic mobility data into ζ–potential was done using Henry's equation.~~(3):~~Results were interpreted as in Pérez et al. (2014)

~~Ue = 2ε ζ *f*(Ka) / 3η (3)~~

~~whereUe is the electrophoretic mobility, ε the dielectric constant, η the sample viscosity and *f*(Ka) the Henry's function.~~

2.2.7. ~~8~~Steady-state fluorescence determinations

Fluorescence spectra for 11S protein and 11S-Bt mixed solutions were determined using a Cary Eclipse fluorescence spectrophotometer (ThermoSpectronic AMINCO-Bowman, Series 2, USA) at 25°C. The spectral resolution for both excitation and emission was 4 nm. Protein intrinsic fluorescence emission spectra corresponding to tryptophan were recorded from 300 to 550 nm with an excitation wavelength of 295 nm. Thus, Bt concentrations evaluated in mixed solutions ranged

from 0.05 to 1%, w/w. Bt fluorescence was also determined under these wavelength range to discard any possible emission of this compound.

2.2.8.~~9~~Binding parameters

Intermolecular interactions of 11S and Bt solutions were detected in the range between 0.05 and 1 %, w/w. These were evaluated from the fluorescence maximum peak of each emission spectra corresponding to mixed solutions in comparison to single 11S spectrum. In general terms, ligand-induced fluorescence quenching might occur through dynamic quenching, i.e. diffusion of free ligand into the distance for fluorescence resonant energy transfer between two fluorophore groups. On the other hand, static quenching could occur in this case the ligand is permanently bound to the protein. The concentration dependence of the fluorescence intensity can be analyzed by Stern-Volmer model (Liang & Subirade, 2010)~~(4)~~(2):

$$F_0/F = 1 + k_q.\ \tau_0\ .[\mathrm{Bt}] = 1 + K.\ [\mathrm{Bt}] \quad \text{~~(4)~~(2)}$$

Where, F0 and F are the fluorescence emission intensities with and without the quencher, respectively; kq is the fluorescence quenching rate constant; τ_0 is the fluorescence lifetime of fluorofore in the absence of quencher; [Bt] is the concentration of betanin, the quencher; and K is the reciprocal of the quencher concentration when the fluorescence intensity decreases by half. A linear plot of F0/F as a function of [Bt] allowed to obtain the K values from the slope of the straight line. τ_0 was reported to be equal 2.9 ns for the Trp residues of 11S at pH 8 (Lakowicz & Weber, 1973). When small molecules are bound independently to a set of equivalent sites on a macromolecule, the equilibrium between free and bound molecules can be expressed by the equation proposed by (Bian, Liu, Tian, & Hu, 2004)~~(5)~~(3):

$$\log (F0 - F)/ F = \log Ka + n.\log[\mathrm{Bt}] \quad \text{~~(5)~~(3)}$$

where, Ka and n are the apparent binding constant and the number of binding sites per 11S molecule, respectively. From the intercept and slope of log (F0-F)/F vs log [Bt], the values adopted by Ka and n can be obtained. The magnitude of the interaction between protein and ligand can be obtained from the Ka value. In addition, the association sites on the protein molecule are indicated by the value acquired by the n parameter (Liang & Subirade, 2010).

The model described by Scatchard (Equation~~5~~6), detailed by (Wei, Xiao, Wang, & Bai, 2010) (6) was the other mathematical approach used here to analyze the binding phenomena between 11S and Bt from fluorescence experimental data.

$$[11S].(1- fi) = [Bt]/n.(1/ fi -1) – (1/n. Ks) \quad (4)$$ ~~(6)~~

$$fi = (fli – flo)/(fl\ max – flo) \quad (5)$$ ~~(7)~~

where, fli is the maximal intensity in each measured point, flo is the maximal intensity without quencher and fl max is the maximal intensity with the highest concentration of quencher; 11S is the protein concentration, Bt is the betanin concentration; Ks and n are the apparent binding constant and the number of binding sites per 11S molecule respectively.

2.2.9. Molecular interactions

Molecular interactions between 11S quinoa globulin and Bt were study by Fourier transform infrared spectra (FTIR) and Differential scanning calorimetry (DSC). The results obtained with the details of the analysis conditions and the devices used can be seen in Supplementary Material.

2.2.10. Loading capacity

The amount of Bt bound to 11S globulin was determined by the difference between the amounts of Bt initially added to the mixed solutions minus the Bt not bound or free Bt (Ochnio et al., 2018). This further refers to the amount of Bt in the supernatant after ultracentrifugation and filtration through a

10 kDa cut off unit (Centricon AmiconR Ultra-4, Millipore, Ireland). 2 mL of each sample, 11S - Bet 0.4% in Tris buffer (assayed at both I=0.5 and I=0.05 M) were centrifuged into the filters. Bt solution was used as a control to determine any Bt loss due to binding to the filter unit. Filters were centrifuged at 4500 x g for 30 min at 24 °C. The flow through was collected and Bt concentration determined. Absorbance at 535nm was measured at 25 ± 1 °C on a UVIKON 943 spectrophotometer (Kontron, Watford, UK). Bt concentration was determined by using a molar absorption coefficient (ε) of 6.5 x 104 $Lmol^{-1}cm^{-1}$ at 536 nm (Gonçalves et al., 2012). Loading capacity for 11S-Bt nanocarriers complexes was determined as:

$$LCBt\ (\%) = [(Bt_N - Bt_S)/Bt_N] \times 100 \qquad (6)$$

Where, Bt_N is the nominal Bt concentration in the system and Bt_S is the Bt concentration after ultracentrifugation and determined by spectrophotometric analysis. The loading capacity was expressed in percentage.

2.2.11.~~10~~ Antioxidant activity of 11S-Bt complexes

ABTS assay

Antioxidant capacity of 11S-Bt nanocomplexes was evaluated by ABTS assay (Re et al., 1999). The pre-formed radical monocation of 2,2′-azinobis-(3-ethylbenzothiazoline-6-sulfonic acid) (ABTS•+) (Merck Millipore, USA), is generated by oxidation of ABTS with potassium persulfate and is reduced in the presence of such hydrogen-donating antioxidants. The influences of both, the concentration of antioxidant and duration of reaction on the inhibition of the radical cation, are taken into account when determining the antioxidant activity. Briefly, ABTS was dissolved in water to a final concentration of 7 mM. Radical cation ABTS•+ was produced by reacting ABTS stock solution with final concentration of potassium persulfate of 2.45 mM and allowing the mixture to stand in darkness at room temperature during 12–16 h before use. The antioxidant activity of 11S-Bt nano-

complexes was determined after ABTS•+ solution was diluted with methanol to an absorbance of 0.80-0.90 at 734 nm, and equilibrated at 30°C. A calibration curve was performed employing galic acid (GA) standards (0–0.012 mg/mL) in methanol. The inhibition of absorbance at 734 nm was calculated.

Ferric reducing antioxidant power (FRAP) assay

FRAP assay was conducted according to the method of Benzie and Strain, 2000 (I.benzie.J.Strain, 2000) with slight modifications. The FRAP reagent contained 5 mL of 10 mM 2,4,6-tripyridy-S-triazine (TPTZ, Sigma-Aldrich Co., St. Louis, MO, USA) solution in 40 mMHCl plus 5 mL of 20 mM FeCl3. 6H2O and 50 mL of 300 mM acetate buffer (pH 3.6) was freshly prepared and warmed at 37°C. Aliquots of 80 μL of 11S, Bt or 11S-Bt nanocarriers or the standard solution of GA (0–0.003 mg/mL) was poured in a test tube, with 520 μL of FRAP reagent solution. The mixture was kept in dark at 25°C for 30 min. The absorbance of the solutions under analysis and different concentrations of GA standard were measured at 593 nm. Finally, the FRAP value was calculated using calibration curve performed employing galic acid (GA) standards in millieQ water.

2.2.12. Statistical analysis

The results were analyzed by two-way ANOVA, $P<0.05$. Analyzes were performed using the statistical program Infostat (FCA, University of Córdoba, Argentina). All the determinations were made at least in triplicate and each reported value represents the mean of independently prepared samples.

3. RESULTS AND DISCUSSION

3.1. 11S isolation and purification

Firstly quinoa flour was obtained by milling. To this end the seeds were ground to flour using a coffee bean grinder (Peabody MC-9100, Argentina). The treatment for flour obtaining consisted in

10 pulses of 15 s each one. The resulting flour was stored in a sealed container at room temperature until use. Quinoa 11S globulin was separated by size exclusion chromatography. Chromatograms obtained firstly revealed a peak corresponding to a high molecular weight (MW) protein (Figure 1 A, black arrow) and other peaks corresponding to smaller polypeptides, possibly, albumins (Burrieza, López-Fernández, & Maldonado, 2014) (Figure 1 A). Secondarily, to improve 11S purification method, we performed its separation with a protocol starting from quinoa flour. The protocol implied the 11S separation from a more intensively milled material which was enriched in protein. Material other than protein had been separated because it stayed attached to the lid grinder during the second stage of milling process. In this case, chromatograms showed the same profile for the high MW protein except that smaller molecular weight polypeptides were almost absent (Figure 1 B). To analyze the identity of the highest MW protein SDS-PAGE were performed. Electrophoresis revealed the typical pattern of 11S with acid and/or basic subunits at 30-35 KDa and 17-20 KDa respectively (Figure 1 C). To confirm the adequateness of the 11S purification process, we evaluated the identity of these bands by MALDI-TOF. In this respect, Supplementary Table 1 summarizes the results obtained when taking into account their description, plant species, theoretical MW and the peptide sequence.

3.2. Protein identification

The MS/MS results confirmed that the main component of 11S-enriched extract was indeed 11S globulin protein. As expected, bands 1 and 2 showed the classical pattern corresponding to the acid and basic fragments of 11S respectively, as we could detect Cqu_c00273.1_g005.1 entry from Quinoa Genome Database. This entry is nearly identical to the 11S protein entries in Uniprot database (Q06AW1_CHEQI and Q06AW2_CHEQI). Interestingly, associated to this previously reported 11S protein, we systematically found Cqu_c03367.1_g006.1, a new member of 11S storage protein family in *Chenopodium quinoa* Willd. (See supplementary Figure 1 – Alignment). Cqu_c03367.1_g006.1 gene product resulted similar to the hypothetical protein of spinach

348 (Spinaceaoleracea L.) SOVF_045250 and to 11S globulin seed storage protein 2 isoform X1 from
349 Beta vulgaris, a predicted 11S globulin (see Supplementary Figure1, NCBI conserved domain
350 (search/Pfam Domains). Besides these main-product bands we also detected and analyzed 2 minor
351 bands. 11S protein was also found in Band 4, which suggests that this band corresponds to a different
352 isoform or a subfraction of 11S globulin.

353 **3.3. Solubility of 11S-Bt nanocarriers**

354 Solubility is one of the most practical indexes of protein denaturation and aggregation and, hence a
355 good indicator of protein functionality (Brinegar & Goundan, 1993; Mäkinen, Zannini, Koehler, &
356 Arendt, 2016). Thus, any improvement in solubility of 11S could impact on its technological
357 applications. Figure 2 shows the solubility variation with the ionic strength, pH 8, for the systems
358 studied. Determinations were performed at I=0.5 M and I=0.05 M.As many globulins from other
359 sources, single 11S increased its solubility at higher I values(Gerzhova, Mondor, Benali, & Aider,
360 2016). Such an increase was also observed upon Bt addition.
361 This finding has enormous importance for processes in which soluble proteins are required as NaCl
362 effect could be offset by Bt. The reason why the ligand increased the 11S solubility should obey to
363 the way in which protein links the smaller Bt molecule and the consequence of such a union on the
364 11S globulin structure. Only a work was found, which gives a description on the molecular
365 phenomena involved in the intermolecular relationship. The authors used the crystal structures for
366 the model soybean enzymes (lipooxygenase and cyclooxygenase), being molecular docking analyses
367 carried out by Vidal, López-Nicolás, Gandía-Herrero, & García-Carmona (2014). This approach
368 allowed getting insight of the betalains binding mode to the active sites of the enzymes. Authors also
369 use AutoDockVina molecular docking software ® which provided a deeper insight into the
370 possibilities indicated before. In the protein with lipooxygenase activity, the guest molecule was
371 docked into the relevant enzyme pocket, possibly via hydrogen bonding interactions. Also the
372 aromatic ring of the pigment accommodated in the pocket close to Ile-257, which may help to

stabilize the overall conformation. In the case of cyclooxigenase, molecular docking analysis with AutoDockVina revealed the interaction of one of the carboxylic groups present in the betalamic acid moiety of a betaxanthin with the side chains of enzyme.

Evidently, Bt would be able to bound to hydrophobic pockets of 11S and to side chains of the macromolecule. Being 11S a multimeric protein, none of these two possibilities could be discarded. The protein solubility increased at I=0.05M to such an extent that no remarkable differences were detected in solution appearance or turbidity in comparison to mixtures at the highest I (conditions of maximum protein solubility, I=0.5M and pH 8). Given the present results, it can be proposed that Bt interferes with the 11S self-assembling mechanism. In turn, the bioactive would interact with each globulin subunit via hydrophobic interactions.

3.4. 11S-Bt molecular interactions. Fluorescence spectroscopy

Fluorescence spectroscopy is an appropriate technique to determine the interaction between ligands and proteins. Many models based on fluorescence quenching of proteins have been used to study the interaction, so more than one model application should be appropriate for the correct analysis of fluorescence quenching (Wei et al., 2010). We applied the Scatchard model to compare the results obtained with the Stern-Volmer model.

11S-Bt interactions were evaluated from their respective fluorescence emission spectra. 11S protein has 12 Trp residues per hexamer (Data obtained from protparam, GenBank: ABI94736.1). It is known that only Trp is able to emit fluorescence when protein solution is excited at 295 nm (Liang & Subirade, 2010). Figure 3 shows the emission spectra for the mixed 11S-Bt solutions, at pH 8 at I=0.5 M in comparison with that of the single protein. It can be seen that at low and high I the maximum florescence intensity values were 5.9 and 5.5 respectively. Under both extreme conditions, results evidenced that the fluorescence intensity decreased as the Bt concentration increased in the bulk solution. In fact, the fluorescence intensity for systems containing the highest Bt concentration

398 decreased approximately 60%. A slight shift towards the red region of the spectrum was detected at
399 the maximum emission wavelength peak, from 334 to 340 nm. Previous reports have claimed that
400 the fluorescence of Trp chromophores changes when they are included in a more hydrophobic
401 environment (Li, Polozova, Gruia, & Feng, 2014; Sandhya, Hegde, Kalanur, Katrahalli, &
402 Seetharamappa, 2011). According to this, Bt linkage to 11S changed subtly the protein structure in
403 solution. The results on intrinsic protein fluorescence quenching, confirm the protein-ligand
404 interaction. To elucidate the type of quenching existing between 11S protein and Bt, the Stern-
405 Volmer and Scatchard models were applied. Supplementary Figure 2 shows the dependence of Fo/F
406 and Bt concentration. The value of Ks, the affinity constant, could be obtained from the slope of the
407 curve. τ_0 acquires a value of 2.9 ns for Trp residues under the conditions used in this study.
408 Therefore, Kq resulted to be equal to $1.85x10^{13}$ and $1.42x10^{13}$ M^{-1} s^{-1}at high and low I, respectively
409 (R^2>0.98 and 0.99). Table 1 indicates that the assumptions for derivation of Equation 3 were
410 satisfactory. The Kq values were much larger than the maximum admitted for dynamic quenching,
411 which is 1.27x1010 $M^{-1}s^{-1}$(Lakowicz& Weber, 1973). These results evidence than the fluorescence
412 intensity changed for 11S after Bt addition and the effect could be attributed to static quenching, i.e.
413 11S-Bt complexes formation. When small molecules have the potential to bind independently to a set
414 of equivalent sites on a macromolecule, the equilibrium between free and bound molecules is given
415 by the Equation 4. This expression allowed to analyze the dependence of fluorescence intensity with
416 Bt concentration for static quenching (Qin, Zhang, Yan, & Ye, 2010). From the plot log [(F0 - F)/F]
417 vs log [Bt] (Stern Volmer model) the n value can be obtained. n relates the number of binding sites
418 on the protein molecule. For Stern Volmer model, n resulted 1.42 and 1.17 for mixtures at I=0.5 M
419 and I=0.05M, respectively. Another parameter to analyze is the apparent binding constant, Ks. The
420 values revealed a strong binding force between 11S and Bt, which was one order of magnitude
421 higher for the higher ionic strength system. Such a result means that the protein manifested a higher

affinity for the Bt and again it could obey to the protein solubility increased under this condition (**Table 1**).

Employing Scatchard model, we obtained Ks value of $1.4x10^5$ for the highest and $7.3x10^4$ for the lowest I, respectively (Table 1). Calculations are exhibited in Supplementary Figure 3. These values kept the trend observed with Stern-Volmer model: the binding force of 11S and Bt was one order of magnitude higher at the highest I. According to the Scatchard model, n parameter resulted 18.18 and 13.77 at high and low I, respectively (Table 1).It is known that the calculated binding sites can result different when different models are considered (Wei et al., 2010), but is important to note that for both models Ks resulted higher when n increased.

435 **3.5. Visualization of Bt binding on the protein by FPLC**

436 Fluorescence analysis strongly suggested that Bt binds to 11S in a stable way via non-covalent
437 unions. With the aim to prove and validate this physical association, another approach was
438 employed. Bt has a known absorption spectra with a peak at λ=536 nm and ε 535=6.5 x 10^4 L mol^{-1}
439 cm^{-1}(Gonçalves et al., 2012) and a MW of 551,48 g/mol, while 11S has a MW of approximately
440 300000 g/mol showing no absorption at λ=536 nm (data not shown). We wonder if we could detect
441 Bt-dependent 536 nm absorbance even when associated with 11S. Employing a size exclusion
442 column (Sephadex® S200 GL 10/300) 11S-Bt complexes were separated from unbound Bt.
443 Absorbance at 536 nm was observed at elusion volume corresponding with 11S, corroborating that
444 Bt was bound to 11S globulin. 11S-Bt nanocarriers eluted at the same volume of 11S
445 (Supplementary Figure 4). That correlates with 11S size and supported the idea that Bt was able to
446 bind 11S and remains linked to the protein in spite of being subjected to size exclusion
447 chromatography (Figure 4). The chromatograms superimposed show the profile of 11S-Bt was
448 coincident with the peak of11S globulin. Interestingly 536 nm absorbance was observed for both 11S
449 globulin (Q06AW1/2 and the new member of 11S globulin family reported in this work;
450 Supplementary Figure 1). Table 2 displays the parameters obtained from chromatographic profile.
451 For instance, the measured area of each peak as mUA * mL at elution volume (Ve) of 11 mL, the
452 area was equal to 156.77mUA * mL and a Ve of 20 mL, the area was121.68mUA * mL.
453
454 **3.6. Analysis of 11S globulin aggregation induced by Bt**
455 Particle size distribution for 11S and 11S-Bt mixed solutions were obtained by DLS. This technique
456 allows gaining insight of the aggregation process for a variety of proteins either to prevent it or to
457 exploit it for specific applications (Ochnio et al., 2018). Several studies have shown that protein
458 unfolding and aggregation can occur depending on protein composition/concentration, pH, I,
459 concentration of ions, fat content, among other factors (Pérez et al., 2014).Thus, focus was put on the

possible 11S aggregation induced by Bt addition as this phenomenon could be a concurrent with complexation with a ligand (Pérez et al., 2014).

Intensity vs particle size showed the oligomeric state, i.e. quaternary structure, of the protein or 11S–Btnano-complexes. At I=0.5 and I=0.05M values, particle size distributions revealed the presence of two populations (Supplementary Figure 5). The first order result from a DLS experiment is an intensity distribution of particle sizes. The intensity distribution is naturally weighted according to the scattering intensity of each particle fraction or family. The fundamental size distribution generated by DLS is an intensity distribution, which could be converted, by the Mie theory, to a volume distribution or a distribution describing the relative proportion of multiple components in the sample based on their mass or volume rather than based on their scattering (Intensity)(Malvern, 2011) . In this context, when the analysis was performed in terms of volume vs size (Figure 5 A and B), only one population resulted to be dominant with a peak at 11 ± 2 nm, expressed in particle diameter.

These data are coincident with the hydrodynamic radius reported previously for trimer of soybean 11S (5.4 nm) and for oat 11S globulin trimers (5.9 nm) as evaluated by DLS (Bojórquez-Velázquez et al., 2016a). The width of the observed peak indicates coexistence of different assembled degrees (Bojórquez-Velázquez et al., 2016b). Differences between pure protein and nano-complexes in terms of particle size distributions were observed. It can be said that Bt addition apparently affect the globulin quaternary structure as smaller sizes were recorded; which would correspond to disassembly of the 11S hexamer. Even more, as can be seen in Figure 5 C, the Z-ave parameter indicated a particle size reduction with Bt addition. This effect seemed to be stronger at low I values. This finding keeps practical importance as 11S-Bt loaded nano-complexes were highly soluble by virtue of the lower particle size after Bt linkage. These results indicated that Bt compensated the NaCl effect on the protein solubility. A comparison of the MW of 11S in presence of Bt was obtained by the protein utility function of Malvern software of DLS appliance (Malvern, 2011) Supplementary

material. This analysis allowed to corroborate that Bt was able to induce disaggregation of the native 11S hexamer (184 ± 13 KDa), manifested by a pentameric form (149 ± 12 KDa) at I=0.5M, meanwhile a tetrameric structure occurred at I=0.05M (119 ± 5 KDa). It can be said that Bt addition could affect quaternary structure, at least at the Bt concentrations here considered. Particle size distribution results were coincident with those obtained with FPLC. The chromatogram corresponding to 11S-Bt nano-complexes eluted at higher volumes or later than the single globulin, which corroborate the hypothesis of protein disaggregation induced by the bioactive.

ζ-potential is a measure of the magnitude of electrostatic interactions between charges at the molecular surface level. These charges can greatly influence particle size distribution, cellular uptake and adsorption to cellular membranes in vivo (Fröhlich, 2012). Therefore, it is a crucial parameter to consider in nanocarriers characterization with potential applications in the food, nutraceutical and cosmetic industries. ζ-potential measurements showed that both 11S and 11S-Bt mixtures presented values that oscillated at around -16 mV (Figure 5, D). Concerning to the nanocarriers, the available literature indicates that electrostatically stabilized hydrocolloids commonly possess ζ-potentials exceeding absolute values of 40 mV (Andreeva et al., 2017). Therefore, the physical stability of nano-complexes does not seem to be only explained by electrostatic stabilization, suggesting that other forces determined the colloidal systems stability. This could arise from steric overlap interaction that keeps11S-Bt nano-complexes separated at an exclusion distance that provides stability to the system.

On the other hand, associative interactions between 11S and Bt had a profound impact on the solubility of nano-complexes as this crucial property resulted equivalent to systems containing the 11S globulin protein at high I. This feature would contribute to the physical stability of this colloidal system delaying precipitation or sedimentation. Associative interactions between 11S and Bt could impart functionality to protein, expanding the food systems in which it could be used, such as

beverages. It is well known that the nanocarriers can behave as delivery systems in specific organs sites, wherewith their antioxidant property could be improved.

3.7. 11S Loading Capacity

The loading capacity of 11S globulin expressed in percentage of Bt resulted equal to 23.36 ± 0.20 and 12.54 ± 0.92, n=2, for I=0.05 and 0.5M, respectively. These results kept correlation with the solubility data exhibited in Figure 2. It can be observed that the increase in solubility could obey to the increase in loading capacity of the protein at low ionic strength. Thus, under this condition (low I), the loading capacity practically doubled that detected at high ionic strength.

3.8. Antioxidant capacity of 11S-Bt nano-complexes.

A structure-activity relationship between betalains and their radical-scavenging properties has been suggested (Gandía-Herrero, Escribano, & García-Carmona, 2010b). The radical-scavenging properties of Bt increases with the number of hydroxyl and imino groups (hydrogen donor). Despite all these advantages, the oral bioavailability of betalains was estimated as rather low, due to the fact that these pigments are degraded when subjected to light, heat, and oxygen (Esatbeyoglu, Wagner, Schini-Kerth, & Rimbach, 2015b; Escribano et al., 2017). With the aim to validate the free radical scavenging capacity of 11S-Bt nanocarriers, we measured the antioxidant activity according to their effect on stable colored solutions of the radical $ABTS^{\bullet+}$. As can be seen in Figure 6 (A and B), single Bt exhibited a higher anti radical capacity at I=0.5M than at I=0.05M and at 0h. This trend was reverted at 24h in the system containing lower salt content, which manifested a higher antioxidant activity. This result could obey to the Bt sensitivity increase at higher salt content. 11S globulin, used as a control in the experiment, also showed anti radical capacity by itself as can be seen in Figure 6B. However, its antioxidant activity did not exceed that registered for 11S-Bt complexes. Thus, $ABTS^{\bullet+}$ radical scavenger capacity was highly increased when Bt was complexed with 11Sglobulin.

534 Antioxidant capacity resulted similar with at I=0.5M and I=0.05M at 0h. The final amount expressed
535 as meq of GA/g of Bt in 11S-Bt complex reached approximately a value of 160, which clearly
536 indicated an additive character when Bt was loaded by 11S protein at both, 0 and 24 h. The
537 expression “additive” was previously used for describing mixed systems presenting a higher value
538 for a specific property than the single components; even the reached value did not exceed the sum of
539 them (Pérez, Carrera Sanchez, Rodriguez Patino, & Pilosof, 2007; Reichert, Salminen, Badolato
540 Bönisch, Schäfer, & Weiss, 2018). Based in these results, we attribute the mentioned additive
541 character of the 11S-Bt complex to the intrinsic antioxidant capacity of 11S.
542 In comparison, it is interesting to note that the polyphenol-dairy proteins interactions have been
543 recently considered to be detrimental to the tea polyphenols antioxidant capacity(Rashidinejad,
544 Birch, Sun-Waterhouse, & Everett, 2017). Thus, this indicates a meaningful difference between
545 polyphenols-protein and Bt-proteins interactions, and merits a complete analysis in order to
546 formulate nano-colloids for bioactive compounds delivery adequately.
547 Several reports describe the antioxidant activity of different peptides (Hartmann & Meisel, 2007;
548 Udenigwe & Aluko, 2012), which could be related to the intrinsic structural characteristics of these
549 macromolecules such as molecular size, hydrophobicity and amino acidic composition. Orsini
550 Delgado et al. (2016) recently analyzed the antioxidant properties of peptides from *Amaranthus*
551 *mantegazzianus*. Such properties were related to the presence of specific amino acids in the
552 polypeptide chain, e.g. Trp, Tyr and Met, which had the highest antioxidant activity followed by
553 Cys, His and Phe. The high antioxidant activity of Trp and Tyr may be explained by their capacity to
554 donate hydrogen. Besides, Met could be oxidized to Metsulfoxide and Cys can donate the sulfur
555 hydrogen (Orsini Delgado et al., 2016). Besides the antiradical activity, the antioxidant capacity of a
556 bioactive compound can be measured through its reducing power, which prevents deleterious
557 oxidative reactions by generating a reducing media. In order to have a complete characterization of
558 the antioxidant capacity of the generated nanocarriers we also analyzed the 11S-Bt complexes

antioxidant capacity by FRAP assay. Figure 7 (A and B) shows in a comparative way the behavior of 11S, Bt and 11S-Bt nano-complexes at I=0.5M and I=0.05M upon time. It is worth to mention that the antioxidant activity of a given compound can vary from method to method depending on factors such as the involved reaction mechanism, antioxidant solubility, oxidation state, pH, and type of oxidation-prone substrate.11S-Bt nanocarrier exhibited an additive character in terms of radical scavengers and reducing power. The possible explanation for this results would be again the synergistic effect mentioned before for 11S-Bt nanocarriers, at both times considered (0 and 24 hs), which would be based on the concomitant antioxidant activity of Bt and the 11S globulin.

4. CONCLUSIONS

In this work a strategy was developed to design and characterize nano-complexes constituted by 11S quinoa seed globulin and Bt. These nano-complexes can serve as vehicles for the bioactive Bt and keeping its health beneficial effects in the presence of light, certain pH and enzymes. We demonstrated that Bt, a natural pigment with antioxidant properties, bounds to extracted and purified 11S quinoa seed globulin. The 11S quinoa globulin identity was verified by MALDI-TOFF approach and *in-silico* analysis. Employing different approaches, we confirmed that Bt interacts with 11S in a stable way. Particle size distribution analysis showed that Bt was not able to induce 11S globulin aggregation. On the contrary, Bt affected the multimeric native protein conformation by induction of disaggregation with the concomitant effect on protein solubility improvement. We observed that as Bt concentration increased the 11S hydrodynamic diameter diminished, indicating a possible conformational change concerning to its quaternary structure specifically affecting the native hexameric form. The nature of such interactions was considered to be principally of physical type. ~~Btcouldbound to 11S on specific sites, i.e. into hydrophobic pockets or on lateral regions, as evaluated by the fluorescence quenching of 11S globulin and by applying different models to the experimental results.~~

584 Higher solubility values were obtained for 11S after nano-complexation, which could be attributed to
585 structural changes of the protein when bound to the bioactive Bt. Higher loading capacity was
586 registered at low ionic strength, which would indicate that the increase in 11S solubility at I=0.05M
587 would be related with the higher amount of Bt loaded. This result may have technological impact as
588 the required amount of NaCl could be diminished to achieve the same protein solubility degree, for
589 instance in nutraceutical formulations. The higher solubility manifested by the nano-complexes has
590 other consequences, the decrease in particle size and the increase in the radical scavenging capacity.
591 These further results may be of physiological importance. Concerning to this, the antioxidant activity
592 of these nano-complexes by two methods: $ABTS^{\bullet+}$, measuring antiradical capacity and FRAP,
593 measuring reducing power. Both methodologies revealed an additive character for 11S-Bt nano-
594 complexes concerning to the antioxidant capacity, in comparison with 11S and Bt individually.
595 Opposite to polyphenols-dairy proteins interactions, Bt preserved its antioxidant capacity after
596 complexation with 11S globulin. Even more, an additive effect with this protein was observed. It is
597 worth to note that for both methods, 11S-Bt and Bt presented higher antioxidant activity at I=0.05M,
598 suggesting that under this condition this property was favorable. These findings, demonstrate that the
599 obtained systems are potentially appropriate as new materials for cosmetic and/or nutraceutical
600 applications.
601 In summary, we are presenting for the first time a new design of nano-biomaterials which were able
602 to maintain Bt antioxidant capacity and combining this beneficial effects with those of the well-
603 known quinoa protein. It can be concluded that the 11S globulin from quinoa seeds was able to
604 protect Bt from oxidation, opening a new perspective in the study of this plant pigment and in the
605 possibility to reinforce their bioactive and antioxidant potential.
606 We have detected the following aspects as important points to perform further investigations, and
607 will be subject of future research: Bt-11S nanocarriers stability towards heat and light effects for the
608 preservation of the bioactive protection, the in-vitro release characteristics in simulated

gastrointestinal fluids. In turn, nanocarriers here designed could be the base for produce more efficacious functional products and to overcome problems as texture modification during process, scarce bioavailability, flavor and nutrients loss.

5. ASSOCIATED CONTENT

Supporting Information

The MS/MS spectra data analysis, multiple sequence alignment. Stern Volmer and Scatchard models application. Protein utilities tool features offered by the Zetananosizer-Zs (Malvern) software. Particle size distribution expressed in terms of Intensity vs size. Molecular interactions study by FTIR and DSC.

6. CONFLICTS OF INTEREST

There are no conflicts to declare.

7. ACKNOWLEDGEMENTS

This research was supported by Projects 20020150100079BA, Universidad de Buenos Aires, ANPCyT (PICTs 2013-1985, 2013-1331 and 2015-3866) and CONICET of Argentina.

8. REFERENCES

Abaee, A., Mohammadian, M., & Jafari, S. M. (2017). Whey and soy protein-based hydrogels and nano-hydrogels as bioactive delivery systems. *Trends in Food Science and Technology, 70*, 69–81. http://doi.org/10.1016/j.tifs.2017.10.011

631 Abugoch, L., Castro, E., Tapia, C., Añón, M. C., Gajardo, P., & Villarroel, A. (2009). Stability of
632 quinoa flour proteins (Chenopodium quinoa Willd.) during storage. *International Journal of*
633 *Food Science and Technology, 44*(10), 2013–2020. http://doi.org/10.1111/j.1365-
634 2621.2009.02023.x

635 Adachi, M., Kanamori, J., Masuda, T., Yagasaki, K., Kitamura, K., Mikami, B., & Utsumi, S.
636 (2003). Crystal structure of soybean 11S globulin: Glycinin A3B4 homohexamer. *Proceedings*
637 *of the National Academy of Sciences, 100*(12), 7395–7400.
638 http://doi.org/10.1073/pnas.0832158100

639 Andreeva, Y. I., Drozdov, A. S., Fakhardo, A. F., Cheplagin, N. A., Shtil, A. A., & Vinogradov, V.
640 V. (2017). The controllable destabilization route for synthesis of low cytotoxic magnetic
641 nanospheres with photonic response. *Scientific Reports, 7*(1), 11343.
642 http://doi.org/10.1038/s41598-017-11673-4

643 Bian, Q., Liu, J., Tian, J., & Hu, Z. (2004). Binding of genistein to human serum albumin
644 demonstrated using tryptophan fluorescence quenching. *International Journal of Biological*
645 *Macromolecules, 34*(5), 275–279. http://doi.org/10.1016/j.ijbiomac.2004.09.005

646 Bois, J. F., Winkel, T., Lhomme, J. P., Raffaillac, J. P., & Rocheteau, A. (2006). Response of some
647 Andean cultivars of quinoa (Chenopodium quinoa Willd.) to temperature: Effects on
648 germination, phenology, growth and freezing. *European Journal of Agronomy, 25*(4), 299–308.
649 http://doi.org/10.1016/j.eja.2006.06.007

650 Bojórquez-Velázquez, E., Lino-López, G. J., Huerta-Ocampo, J. A., Barrera-Pacheco, A., Barba de
651 la Rosa, A. P., Moreno, A., … Osuna-Castro, J. A. (2016a). Purification and biochemical
652 characterization of 11S globulin from chan (Hyptis suaveolens L. Poit) seeds. *Food Chemistry,*
653 *192,* 203–211. http://doi.org/10.1016/j.foodchem.2015.06.099

Bojórquez-Velázquez, E., Lino-López, G. J., Huerta-Ocampo, J. A., Barrera-Pacheco, A., Barba de la Rosa, A. P., Moreno, A., … Osuna-Castro, J. A. (2016b). Purification and biochemical characterization of 11S globulin from chan (Hyptis suaveolens L. Poit) seeds. *Food Chemistry*, *192*, 203–211. http://doi.org/10.1016/j.foodchem.2015.06.099

Brinegar, C., & Goundan, S. (1993). Isolation and characterization of chenopodin, the 11S seed storage protein of quinoa (Chenopodium quinoa). *Journal of Agricultural and Food Chemistry*, *41*(2), 182–185. http://doi.org/10.1021/jf00026a006

Burrieza, H. P., Koyro, H.-W., Tosar, L. M., Kobayashi, K., & Maldonado, S. (2012). High salinity induces dehydrin accumulation in Chenopodium quinoa Willd. cv. Hualhuas embryos. *Plant and Soil*, *354*(1–2), 69–79. http://doi.org/10.1007/s11104-011-1045-y

Burrieza, H. P., López-Fernández, M. P., & Maldonado, S. (2014). Analogous reserve distribution and tissue characteristics in quinoa and grass seeds suggest convergent evolution. *Frontiers in Plant Science*, *5*. http://doi.org/10.3389/fpls.2014.00546

Esatbeyoglu, T., Wagner, A. E., Schini-Kerth, V. B., & Rimbach, G. (2015a). Betanin--a food colorant with biological activity. *Molecular Nutrition & Food Research*, *59*(1), 36–47. http://doi.org/10.1002/mnfr.201400484

Esatbeyoglu, T., Wagner, A. E., Schini-Kerth, V. B., & Rimbach, G. (2015b). Betanin--a food colorant with biological activity. *Molecular Nutrition & Food Research*, *59*(1), 36–47. http://doi.org/10.1002/mnfr.201400484

Escribano, J. (1998). Characterization of the antiradical activity of betalains from Beta vulgaris L. roots. *Phytochemical Analysis*, *9*(3), 124–127. http://doi.org/10.1002/(SICI)1099-1565(199805/06)9:3<124::AID-PCA401>3.0.CO;2-0

Escribano, J., Cabanes, J., Jiménez-Atiénzar, M., Ibañez-Tremolada, M., Gómez-Pando, L. R.,

García-Carmona, F., & Gandía-Herrero, F. (2017). Characterization of betalains, saponins and antioxidant power in differently colored quinoa (Chenopodium quinoa) varieties. *Food Chemistry*, *234*, 285–294. http://doi.org/10.1016/j.foodchem.2017.04.187

Faridi Esfanjani, A., & Jafari, S. M. (2016). Biopolymer nano-particles and natural nano-carriers for nano-encapsulation of phenolic compounds. *Colloids and Surfaces B: Biointerfaces*, *146*, 532–543. http://doi.org/10.1016/j.colsurfb.2016.06.053

Fröhlich, E. (2012). The role of surface charge in cellular uptake and cytotoxicity of medical nanoparticles. *International Journal of Nanomedicine*, 5577. http://doi.org/10.2147/IJN.S36111

Gan, Q., & Wang, T. (2007). Chitosan nanoparticle as protein delivery carrier—Systematic examination of fabrication conditions for efficient loading and release. *Colloids and Surfaces B: Biointerfaces*, *59*(1), 24–34. http://doi.org/10.1016/j.colsurfb.2007.04.009

Gandía-Herrero, F., Escribano, J., & García-Carmona, F. (2010a). Structural implications on color, fluorescence, and antiradical activity in betalains. *Planta*, *232*(2), 449–60. http://doi.org/10.1007/s00425-010-1191-0

Gandía-Herrero, F., Escribano, J., & García-Carmona, F. (2010b). Structural implications on color, fluorescence, and antiradical activity in betalains. *Planta*, *232*(2), 449–60. http://doi.org/10.1007/s00425-010-1191-0

Gerzhova, A., Mondor, M., Benali, M., & Aider, M. (2016). Study of total dry matter and protein extraction from canola meal as affected by the pH, salt addition and use of zeta-potential/turbidimetry analysis to optimize the extraction conditions. *Food Chemistry*, *201*, 243–252. http://doi.org/10.1016/j.foodchem.2016.01.074

Gonçalves, L. C. P., Trassi, M. A. de S., Lopes, N. B., Dörr, F. A., Santos, M. T. dos, Baader, W. J., … Bastos, E. L. (2012). A comparative study of the purification of betanin. *Food Chemistry*,

131(1), 231–238. http://doi.org/10.1016/j.foodchem.2011.08.067

Hartmann, R., & Meisel, H. (2007). Food-derived peptides with biological activity: from research to food applications. *Current Opinion in Biotechnology*, *18*(2), 163–9. http://doi.org/10.1016/j.copbio.2007.01.013

Huang, Q., Yu, H., & Ru, Q. (2010). Bioavailability and Delivery of Nutraceuticals Using Nanotechnology. *Journal of Food Science*, *75*(1), R50–R57. http://doi.org/10.1111/j.1750-3841.2009.01457.x

I.benzie.J.Strain. (2000). The ferric reducing ability of plasma as a measure of antioxodant. *Analytical Biochemistry*, *239*(1), 70–76.

Ichikawa, S., Iwamoto, S., & Watanabe, J. (2005). Formation of biocompatible nanoparticles by self-assembly of enzymatic hydrolysates of chitosan and carboxymethyl cellulose. *Biosci Biotechnol Biochem*, *69*(9), 1637–1642. http://doi.org/10.1271/bbb.69.1637

Iswaran, V., & Marwah, T. S. (1980). A modified rapid Kjeldahl method for determination of total nitrogen in agricultural and biological materials. *Geobios*, *7*(6), 281–282.

Jacobsen, S.-E., Mujica, A., & Jensen, C. R. (2003). The Resistance of Quinoa (Chenopodium quinoa Willd.) to Adverse Abiotic Factors. *Food Reviews International*, *19*(1–2), 99–109. http://doi.org/10.1081/FRI-120018872

Jafari, S. M., & McClements, D. J. (2017). *Nanotechnology Approaches for Increasing Nutrient Bioavailability*. *Advances in Food and Nutrition Research* (1st ed., Vol. 81). Elsevier Inc. http://doi.org/10.1016/bs.afnr.2016.12.008

Laemmli, U. K. (1970). Cleavage of structural proteins during the assembly of the head of bacteriophage T4. *Nature*, *227*(5259), 680–685. http://doi.org/10.1038/227680a0

722 Lakowicz, J. R., & Weber, G. (1973). Quenching of fluorescence by oxygen. A probe for structural
723 fluctuations in macromolecules. *Biochemistry*, *12*(21), 4161–70. Retrieved from
724 http://www.ncbi.nlm.nih.gov/pubmed/4795686

725 Li, Y., Polozova, A., Gruia, F., & Feng, J. (2014). Characterization of the degradation products of a
726 color-changed monoclonal antibody: tryptophan-derived chromophores. *Analytical Chemistry*,
727 *86*(14), 6850–7. http://doi.org/10.1021/ac404218t

728 Liang, L., & Subirade, M. (2010). β-Lactoglobulin/Folic Acid Complexes: Formation,
729 Characterization, and Biological Implication. *The Journal of Physical Chemistry B*, *114*(19),
730 6707–6712. http://doi.org/10.1021/jp101096r

731 Mäkinen, O. E., Zannini, E., Koehler, P., & Arendt, E. K. (2016). Heat-denaturation and aggregation
732 of quinoa (Chenopodium quinoa) globulins as affected by the pH value. *Food Chemistry*, *196*,
733 17–24. http://doi.org/10.1016/j.foodchem.2015.08.069

734 Malvern, I. (2011). Inform White Paper Dynamic Light Scattering. *Malvern Guides*, 1–6.

735 Nasti, A., Zaki, N. M., de Leonardis, P., Ungphaiboon, S., Sansongsak, P., Rimoli, M. G., & Tirelli,
736 N. (2009). Chitosan/TPP and Chitosan/TPP-hyaluronic Acid Nanoparticles: Systematic
737 Optimisation of the Preparative Process and Preliminary Biological Evaluation. *Pharmaceutical*
738 *Research*, *26*(8), 1918–1930. http://doi.org/10.1007/s11095-009-9908-0

739 Neuhoff, V., Arold, N., Taube, D., & Ehrhardt, W. (1988). Improved staining of proteins in
740 polyacrylamide gels including isoelectric focusing gels with clear background at nanogram
741 sensitivity using Coomassie Brilliant Blue G-250 and R-250. *Electrophoresis*, *9*(6), 255–262.
742 http://doi.org/10.1002/elps.1150090603

743 Nishinari, K., Fang, Y., Guo, S., & Phillips, G. O. (2014). Soy proteins: A review on composition,
744 aggregation and emulsification. *Food Hydrocolloids*, *39*, 301–318.

http://doi.org/10.1016/j.foodhyd.2014.01.013

Nowak, V., Du, J., & Charrondière, U. R. (2016). Assessment of the nutritional composition of quinoa (Chenopodium quinoa Willd.). *Food Chemistry*, *193*, 47–54. http://doi.org/10.1016/j.foodchem.2015.02.111

Ochnio, M., Martínez, J., Allievi, M., Palavecino, M., Martínez, K., & Pérez, O. (2018). Proteins as Nano-Carriers for Bioactive Compounds. The Case of 7S and 11S Soy Globulins and Folic. *Polymers*, *10*(2), 149. http://doi.org/10.3390/polym10020149

Orsini Delgado, M. C., Nardo, A., Pavlovic, M., Rogniaux, H., Añón, M. C., & Tironi, V. A. (2016). Identification and characterization of antioxidant peptides obtained by gastrointestinal digestion of amaranth proteins. *Food Chemistry*, *197*, 1160–1167. http://doi.org/10.1016/j.foodchem.2015.11.092

Park, J. H., Lee, Y. J., Kim, Y. H., & Yoon, K. S. (2017). Antioxidant and Antimicrobial Activities of Quinoa (Chenopodium quinoa Willd .) Seeds Cultivated in Korea, *22*(August), 195–202. http://doi.org/10.3746/pnf.2017.22.3.195

Pedreño, M. A., & Escribano, J. (2001). Correlation between antiradical activity and stability of betanine from Beta vulgaris L roots under different pH, temperature and light conditions. *Journal of the Science of Food and Agriculture*, *81*(7), 627–631. http://doi.org/10.1002/jsfa.851

Pérez, O., Carrera Sanchez, C., Rodriguez Patino, J., & Pilosof, A. (2007). Adsorption dynamics and surface activity at equilibrium of whey proteins and hydroxypropyl–methyl–cellulose mixtures at the air-water interface. *Food Hydrocolloids*, *21*(5–6), 794–803. http://doi.org/10.1016/j.foodhyd.2006.11.013

Pérez, O., David-Birman, T., Kesselman, E., Levi-Tal, S., & Lesmes, U. (2014). Milk protein–vitamin interactions: Formation of beta-lactoglobulin/folic acid nano-complexes and their

768 impact on in vitro gastro-duodenal proteolysis. *Food Hydrocolloids*, *38*, 40–47.
769 http://doi.org/10.1016/j.foodhyd.2013.11.010

770 Qin, Y., Zhang, Y., Yan, S., & Ye, L. (2010). A comparison study on the interaction of hyperoside
771 and bovine serum albumin with Tachiya model and Stern-Volmer equation. *Spectrochimica*
772 *Acta. Part A, Molecular and Biomolecular Spectroscopy*, *75*(5), 1506–10.
773 http://doi.org/10.1016/j.saa.2010.02.007

774 Quiroga, A. V., Martínez, E. N., & Añón, M. C. (2007). Amaranth globulin polypeptide
775 heterogeneity. *Protein Journal*, *26*(5), 327–333. http://doi.org/10.1007/s10930-007-9075-2

776 Rashidinejad, A., Birch, E. J., Sun-Waterhouse, D., & Everett, D. W. (2017). Addition of milk to tea
777 infusions: Helpful or harmful? Evidence from in vitro and in vivo studies on antioxidant
778 properties. *Critical Reviews in Food Science and Nutrition*, *57*(15), 3188–3196.
779 http://doi.org/10.1080/10408398.2015.1099515

780 Re, R., Pellegrini, N., Proteggente, A., Pannala, A., Yang, M., & Rice-Evans, C. (1999). Antioxidant
781 activity applying an improved ABTS radical cation decolorization assay. *Free Radical Biology*
782 *& Medicine*, *26*(9–10), 1231–7.

783 Reichert, C. L., Salminen, H., Badolato Bönisch, G., Schäfer, C., & Weiss, J. (2018). Concentration
784 effect of Quillaja saponin – Co-surfactant mixtures on emulsifying properties. *Journal of*
785 *Colloid and Interface Science*, *519*, 71–80. http://doi.org/10.1016/j.jcis.2018.01.105

786 Ruiz, G. A., Xiao, W., Van Boekel, M., Minor, M., & Stieger, M. (2016). Effect of extraction pH on
787 heat-induced aggregation, gelation and microstructure of protein isolate from quinoa
788 (Chenopodium quinoa Willd). *Food Chemistry*, *209*, 203–210.
789 http://doi.org/10.1016/j.foodchem.2016.04.052

790 Sanchez, H. B., Lemeur, R., Damme, P. Van, & Jacobsen, S.-E. (2003). Ecophysiological Analysis

Of Drought And Salinity Stress Of Quinoa (Chenopodium Quinoa willd.). *Food Reviews International*, *19*(1–2), 111–119. http://doi.org/10.1081/FRI-120018874

Sandhya, B., Hegde, A. H., Kalanur, S. S., Katrahalli, U., & Seetharamappa, J. (2011). Interaction of triprolidine hydrochloride with serum albumins: thermodynamic and binding characteristics, and influence of site probes. *Journal of Pharmaceutical and Biomedical Analysis*, *54*(5), 1180–6. http://doi.org/10.1016/j.jpba.2010.12.012

Strack, D., Vogt, T., & Schliemann, W. (2003). Recent advances in betalain research. *Phytochemistry*, *62*(3), 247–69. Retrieved from http://www.ncbi.nlm.nih.gov/pubmed/12620337

Tang, Y., Li, X., Chen, P. X., Zhang, B., Hernandez, M., Zhang, H., … Tsao, R. (2015). Characterisation of fatty acid, carotenoid, tocopherol/tocotrienol compositions and antioxidant activities in seeds of three Chenopodium quinoa Willd. genotypes. *Food Chemistry*, *174*, 502–508. http://doi.org/10.1016/j.foodchem.2014.11.040

Tang, Y., Li, X., Zhang, B., Chen, P. X., Liu, R., & Tsao, R. (2015). Characterisation of phenolics, betanins and antioxidant activities in seeds of three Chenopodium quinoa Willd. genotypes. *Food Chemistry*, *166*, 380–388. http://doi.org/10.1016/j.foodchem.2014.06.018

Udenigwe, C. C., & Aluko, R. E. (2012). Food protein-derived bioactive peptides: production, processing, and potential health benefits. *Journal of Food Science*, *77*(1), R11-24. http://doi.org/10.1111/j.1750-3841.2011.02455.x

Vidal, P. J., López-Nicolás, J. M., Gandía-Herrero, F., & García-Carmona, F. (2014). Inactivation of lipoxygenase and cyclooxygenase by natural betalains and semi-synthetic analogues. *Food Chemistry*, *154*, 246–54. http://doi.org/10.1016/j.foodchem.2014.01.014

Wada H, Masumoto-Kubo C1, Gholipour Y, Nonami H, Tanaka F, Erra-Balsells R, Tsutsumi K, Hiraoka K, M. S. (2014). Rice chalky ring formation caused by temporal reduction in starch

biosynthesis during osmotic adjustment under foehn-induced dry wind. *PLoS ONE*.

Wei, X. L., Xiao, J. B., Wang, Y., & Bai, Y. (2010). Which model based on fluorescence quenching is suitable to study the interaction between trans-resveratrol and BSA? *Spectrochimica Acta. Part A, Molecular and Biomolecular Spectroscopy*, *75*(1), 299–304. http://doi.org/10.1016/j.saa.2009.10.027

Yasui, Y., Hirakawa, H., Oikawa, T., Toyoshima, M., Matsuzaki, C., Ueno, M., … Fujita, Y. (2016). Draft genome sequence of an inbred line of Chenopodium quinoa , an allotetraploid crop with great environmental adaptability and outstanding nutritional properties. *DNA Research*, *23*(6), 535–546. http://doi.org/10.1093/dnares/dsw037

Legends for Figures

Figure 1. Elusion profile by FPLC of 11S extracted from quinoa flour after first milling **A** and thesecond milling **B.** FPLC conditions: Column Sephadex S200 10/300 GL, pH 8, 0.5 M of NaCl and 25°C**. SDS-PAGE.** Lane a: quinoa extract before chromatography. Lane b and c: Subunits of 11S of 30 and 20 kDa (1 & 2 respectively). Lane d: this band would correspond to an 11S B and a hypothetical protein SOVF_045250 determined by *in silico* analysis.

Figure 2. Solubility of 11S-Bt nano-carriers. Conditions of the essay: mixing ratio: 11S 0.1: Bt1, *I*=0.5M and *I*=0.05M, pH 8.Mean ± SD, n=4. Means with the same letter represent not significative differences ($p>0.05$).

Figure 3: Fluorescence emission spectra of quinoa 11S globulin 0.1%, w/w, in the presence of various concentrations of Bt (0.05, 0.1, 0.2, 0.3, 0.4, 0.6, 0.8 and 1% w/w), pH 8. **A**: *I*=0.5M and B: *I*=0.05M. λex=295 nm.

Figure 4. Analysis of Bt-11S binding by Size Exclusion Chromatography. Chromatograms at λ=280nm for 11S and 11S-Bt. Arrows indicate the respective peaks of 11S and 11S-Bt.

Figure 5. Particle size distribution for 11S 0.1% and 11S-Bt ([Bt]=0.05, 0.1, 0.2 0.3, 0.4, 0.6, 0.8 and 1% w/w); *I*=0.5 M (**A**) and *I*=0,05M (**B**) **.** Z-ave for systems with 0% and 1% w/w of Bt at different *I* (**C**). ζ-potential variation for 11S and 11S-Bt nano-complexes at Bt used in A and B (**D**). Mean ± SD, n=10. Means with the same letter represent not significative differences ($p>0.05$).

Figure 6. Anti-radical activity as evaluated by the ABTS assay for 11S, Bt or 11S-Bt nano-carriers (11S: Bt = 0.1:1). Time=0 h (A) and 24h (B).*I*=0.5 M and *I*=0,05M. Mean ± SD, n=3. Means with the same letter represent not significative differences ($p>0.05$).

Figure 7. Antioxidant activity as evaluated by the FRAP assay for 11S, Bt or 11S-Bt nano-complexes (11S: Bt = 0.1:1). Time= 0 h (A) and 24h (B). *I*=0.5 M and *I*=0,05M. Mean ± SD, n=3. Means with the same letter represent not significative differences ($p>0.05$).

Table 1. Binding parameters derived from the Stern Volmer and Scatchard models application on experimental data of 11S-Bt nano-complexes fluorescence. ND: not determined as the model did not contemplate it.

11S-Bt			
Stern Volmer model			
NaCl(M)	**Kq (M^{-1} S^{-1})**	**Ks (M^{-1})**	***n***
0.5	**1.85×10^{13}**	**3.8×10^{6}**	**1.42**
0	**1.42×10^{13}**	**2.5×10^{5}**	**1.17**
Scatchard model			
NaCl(M)	**Kq (M^{-1} S^{-1})**	**Ks (M^{-1})**	***n***
0.5	**ND**	**1.4×10^{5}**	**18.18**
0	**ND**	**7.3×10^{4}**	**13.77**

Table 2. Peaks area for 11S-Bt nano-complexes and free Bt. λ=280 nm is the maximal absorbance for 11S and 11S-Bt nano-complexes. Ve= elution volume. Values <0.05 mUA*mL indicate absence of signal.

Absorbance λ=280 nm		
Sample	**Ve 10-13mL**	**Ve 20 mL**
11S	**140**	**5.03**
Bt	**<0.05**	**107.4**
11S-Bt	**156.77**	**121.68**

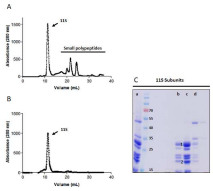

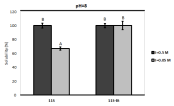

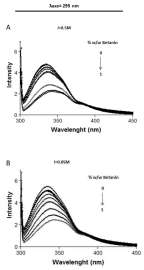

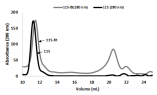

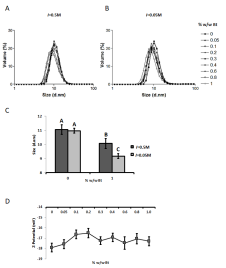

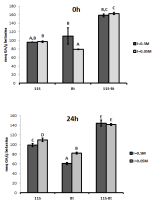

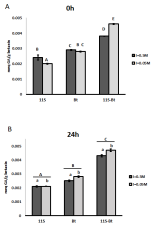

Highlights

A new bionano-carrier was designed based 11S quinoa globulin and betanin.

Betanin increased 11S solubility with no salt added.

Florescence parameters that characterize 11S-Bt interactions were obtained

11S quinoa globulin suffer disaggregation after complexation with Bt

11S-Bt loaded nanocarriers increased the antioxidant capacity of the bioactive